SUPPORT-FREE INFILTRATION OF SELECTIVE LASER SINTERED (SLS) SILICON CARBIDE PREFORMS

B.Y. Stevinson, D.L. Bourell, J.J. Beaman Jr.,
Mechanical Engineering Department, Laboratory for Freeform Fabrication, The University of Texas at Austin, 1 University Station, C2200, Austin TX USA 78712-0292
Reviewed, accepted September 14, 2006

Abstract

Non-metallic objects are often difficult to manufacture due to high melting temperatures, poor sinterability, limited ductility, and difficulty in machining. Freeform fabrication techniques coupled with liquid infiltration offer a cost-effective and rapid manufacturing mechanism for composite parts with complex geometry and adequate properties. Selective laser sintered (SLS) silicon carbide (SiC) preforms infiltrated with liquid silicon develop localized infiltrant over-extrusions onto surfaces and at surface irregularities. Several shrinkage mechanisms including densification were studied as possible causes of these overfilling extrusions, and the results are discussed below. This research was supported by NSF Grant Number DMI-0522176.

1. Background

Reaction bonded silicon carbide (RBSiC) is an engineering ceramic that can be formed by densifying porous silicon carbide preforms with silicon carbide produced in situ via chemical reaction between silicon and carbon. These materials are of interest where high temperature strength and stability are required. Applications include electronics processing wafer carriers and boats, kiln components, and wear parts. Selective laser sintering with subsequent liquid infiltration provides a cost-effective and relatively easy manufacturing route for RBSiC, and permits a generous freedom of design. In support-free selective laser sintering, phenolic and silicon carbide powders are mixed and loaded into an SLS machine. A computer-controlled scanning laser guided by an .stl file melts a shape into a thin layer of the powder. A new layer of powder is rolled on top of this and the process repeats, creating a 3-dimensional part. Only the phenolic is melted under the laser, and it binds the silicon carbide particles together to create a green part. Figure 1 shows a schematic of the SLS process.

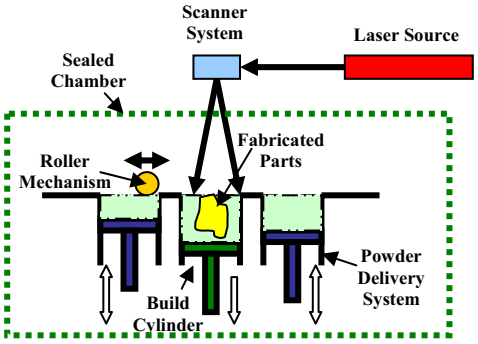

Figure 1: Schematic of Selective Laser Sintering Process

The green part is heated in vacuum to carbonize the binder, thus creating a "brown part" which is further heated in the presence of silicon pellets to induce liquid silicon infiltration. Favorable surface energy conditions, low viscosity, and other parameters allow the molten silicon to quickly and fully infiltrate the porous brown part. In the process, silicon reacts with the carbon

to form new silicon carbide, i.e. reaction bonded silicon carbide. The net result is a fully dense composite part of silicon and silicon carbide.

Pressureless infiltration of silicon into the silicon carbide preform is driven by surface capillary forces, which requires among other things a wetting angle $\theta < 90°$ and favorable surface free energies. Based on Washburn's relationship for the driving pressure P on a liquid drawing up a tube, Cornie and co-workers developed a threshold pressure for spontaneous infiltration P* into a porous medium (Mortensen and Cornie, 1987; Oh, et al., 1989):

$$P^* = \frac{6\lambda(-\gamma_{lv}\cos\theta)\Delta}{(1-\Delta)D} \tag{1}$$

where λ is the ratio of the particle actual surface area to the surface area of a sphere of identical volume, γ_{lv} is the liquid surface free energy, Δ is the relative density and D is the particle size.

The equilibrium height of liquid h_{max} infiltrating into a porous medium and working against gravity in pressureless infiltration has been derived (Gern, 1995):

$$h_{\max} = \frac{2\gamma_{lv}\cos\theta}{rg\rho} \tag{2}$$

where g is the acceleration due to gravity and ρ is the molten infiltrant density.

Applying Equation 1 to silicon infiltration into a silicon carbide preform, the following parameters may be taken (Wang, 1999): $\lambda = 1.3$, $\gamma_{lv} = 846$ mJ/m^2, $\Delta = 0.4$ and D = 40 μm. The threshold pressure P* is calculated to be -83kPa. This is effectively a vacuum drawing molten silicon into the pore structure. The maximum height of silicon infiltration into a silicon carbide preform may be calculated using Equation 2 with additional parameters $\theta = 41°$, r = 20 μm, g = 9.8 m/s^2 and $\rho = 2.65$ g/cm^3. The result, 2.5 m, is comparable to 2 m obtained by Gern (1995). Based on this information, one might expect silicon to readily infiltrate silicon carbide preforms.

2. Experimental

Commercial grade -280 grit silicon carbide (SiC) powder provided by Industrial Supply, Inc., and GP-5546 phenolic resin from Georgia Pacific Resins, Inc. that was further milled to 11μm, were mixed in a respective 100:10 weight ratio. After 5 hours of mixing in a cement mixer, the powder was selective laser sintered in a 3D Systems Sinterstation 2000. The Sinterstation 2000 operating parameters were as follows: laser power, 10W; outline laser power, 4W; layer thickness, 75 μm; scan spacing, 100 μm; part bed temperature, 75°C; scan speed, 1.3 m/s; beam diameter, 450 μm; and nitrogen process gas was used. After sintering, the green parts were removed from the Sinterstation and infiltrated with BJB TC-1622 A/B epoxy mixed with xylene in a 1:1 ratio to reduce the viscosity. They were then post-cured according to the manufacturer's recommendations. Next, the parts were placed in a boron nitride coated graphite crucible in indirect contact with silicon pellets, Figure 2. Using a high temperature graphite vacuum furnace, the parts were heated with the following temperature profile: 180°C/hr from room temperature to 200°C, 30°C/hr to 500°C during which the phenolic and epoxy decomposed, 300°C/hr to 1400°C, 500°C/hr to 1650°C, and then immediately furnace cooled. Cooling time was approximately 7 hours. The furnace was backfilled with argon before furnace processing under vacuum, and argon was pulsed through the furnace chamber during processing to sweep away byproducts of the phenolic decomposition and other chemical reactions.

Figure 2: Furnace setup showing part in indirect contact with silicon pellets

Parts of various geometries were created to characterize the overfilling. Bulk and fracture surfaces of the parts were examined using scanning electron microscopy (SEM).

For densification studies, five 25mm cubes were created using the above pre-furnace processes. These cubes were weighed and measured with a calibrated digital micrometer (±2.5μm) at 15 locations each after five processing points, for a total of 75 measurements per processing point. Measurements were taken after: SLS processing (as green parts), epoxy infiltration, conversion to brown part up to 800°C (30°C/hr from room temperature to 500°C and then 300°C to 800°C), heating to 1650°C (250°C/hr from room temperature to 1400°C and then 500°C/hr to 1650°C), and silicon infiltration to 1650°C (250°C/hr from room temperature to 1400°C and then 500°C/hr to 1650°C). Parts were allowed to cool completely between steps to eliminate the influence of thermal expansion on the measurements. In addition to the physical experiments, an Ashby densification plot based on information from German (1998) was constructed for pressureless silicon carbide heating.

3. Results and Discussion

SEM fracture surface images taken of the green part, Figure 3a, and after brown part conversion, Figure 3b, confirm that the phenolic bridges between the silicon carbide particles convert to carbon ligaments after heat treatment. The carbon ligaments are visible in the center of Figure 3b.

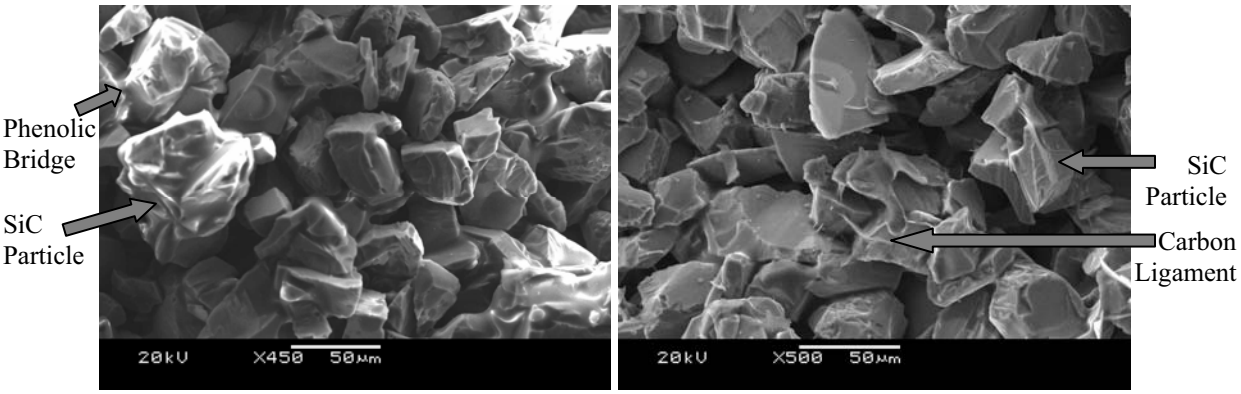

Figure 3: SEM image of green part (a) and brown part heated to 800°C (b)

SEM and optical microscope images taken of silicon infiltrated parts verify that the resulting parts are fully dense silicon-silicon carbide composites, Figures 4a and 4b. Figure 4a is a fracture surface image, and Figure 4b is a diamond saw-cut cross-sectional view.

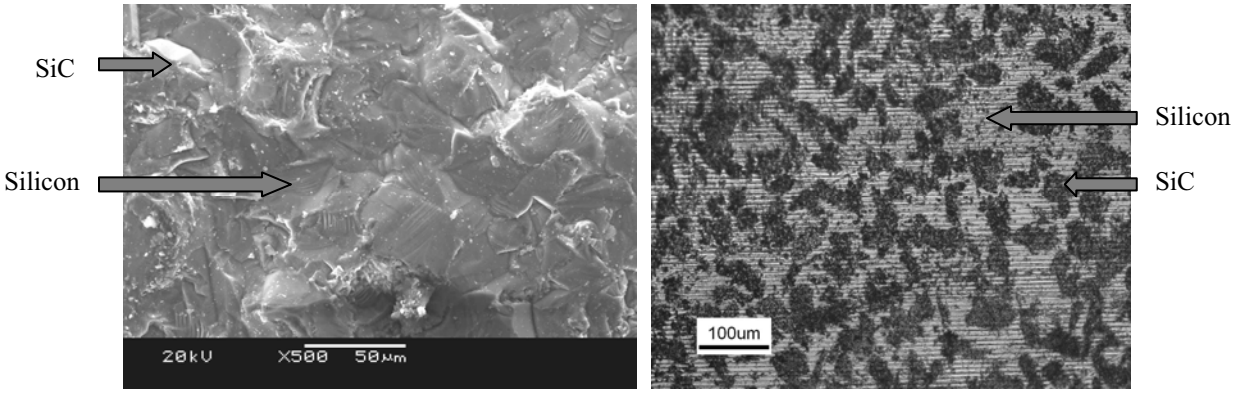

(a) (b)

Figure 4: SEM image (a) and optical micrograph (b) of silicon infiltrated part, heated to 1650°C

Surface defects on the parts occurred as two forms of overfilling: macroscopic overfilling at geometrical stress concentrations (Figure 5), and microscopic overfilling at bulk surfaces (Figure 6). The microscopic overfills are present as small hemispherical protrusions of silicon spread more or less uniformly over the surface of the part. These protrusions are 100 µm to 2 mm in diameter, and they generally occupy the surface at a frequency on the order of 6-10 protrusions per cm^2. While the macroscopic overfilling can be explained as the result of the molten silicon flow being driven into areas of high stress concentrations, the microscopic overfilling on the bulk surfaces is not as intuitive and is the primary focus of this investigation.

Figure 5: Macroscopic Overfilling at Geometrical Stress Concentrations

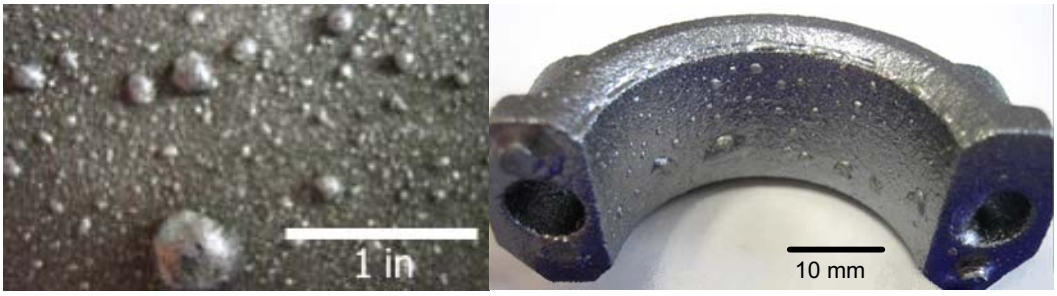

Figure 6: Microscopic Overfilling on Bulk Surfaces

Shrinkage of the silicon carbide matrix during the liquid silicon phase was thought to be the cause of the microscopic overfilling. Once the preform is completely infiltrated, any shrinkage of the matrix could presumably force molten silicon out onto the surface. From calculations based on the average amount of overfilling observed in the parts, it was determined that only a small amount of shrinkage in the silicon carbide matrix was needed to produce the observed amount of overfilling. This measured volume change in the silicon carbide, $\Delta V/V$, is approximately -(5 to 6)%, or an equivalent dimensional change $\Delta L/L$ of approximately -1.5% to -2%. Alternatively, this is effectively a change in relative density ρ/ρ_{th} from 0.5 to 0.53. Three causes of shrinkage were explored. First, thermal contraction during silicon solidification was considered. Silicon has a lower coefficient of thermal expansion (CTE) than silicon carbide and would therefore be under compression during cooling, but the difference in volumetric changes between the two materials is vastly insufficient to cause the experimentally observed amount of overfilling. The second consideration was the formation of new silicon carbide from the reaction

$$Si_{(l)} + C_{(s)} \rightarrow SiC_{(s)} \tag{3}$$

But the silicon carbide formed in the reaction occupies much greater volume than the precursor carbon did, so the material experiences a net expansion, not contraction as needed to explain the overfilling mechanism. This is seen from simple molar volume calculations. Finally, light densification of the silicon carbide during heating was considered. Construction of an Ashby densification map (Figure 7) predicted virtually no densification within the temperatures, time, and pressures used in part processing. Although densification is significant when high process pressures are used (Dutta, 1989), under vacuum no densification occurs.

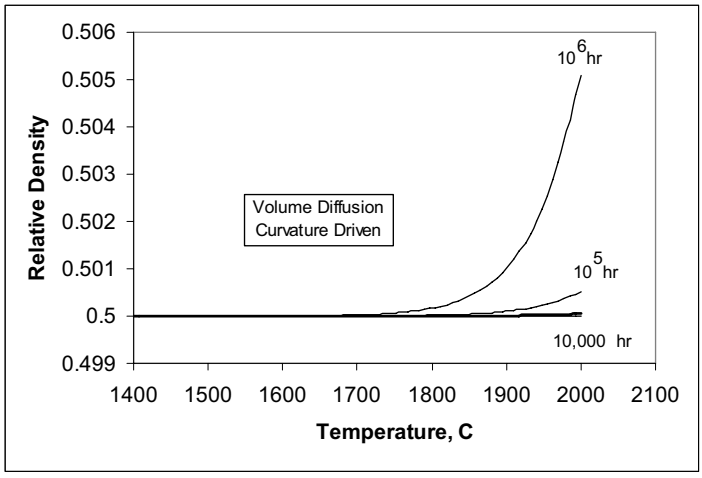

Figure 7: Ashby Densification Map of SiC in vacuum

Furthermore, data from the five 25mm cubes indicated that while shrinkage occurred during the temperature range 200-1400°C, none occurred during the temperature range 1400-1650°C in which silicon infiltration and solidification occurred (Figure 8). The shrinkage during the lower temperatures can be attributed to the expected mass loss during phenolic and epoxy decomposition, which is significant in the temperature range 400-700°C (Ko, 2000). Finally, microscopic overfilling was observed after parts had been "pre-densified," i.e. they were heated to 1650°C without silicon and then reheated to 1650°C with silicon infiltration. Virtually all densification would have taken place during the first step, thus eliminating overfilling during the second step.

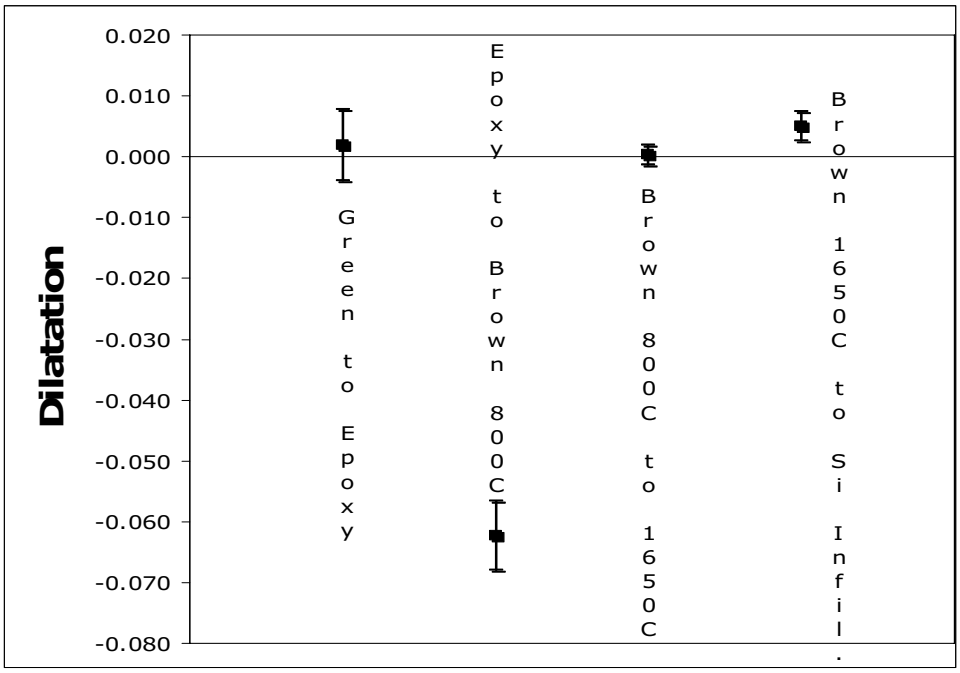

Figure 8: Dilatation Between Processing Steps of SLS Si-SiC Parts

4. Conclusions

Using selective laser sintering and liquid silicon infiltration, fully dense reaction bonded silicon carbide parts have been successfully created. However, the superficial extrusions created in the process must be eliminated before it is of serious commercial value for this material system. These extrusions are difficult to remove using bead blasting, and the process is more cost-effective without post-process finishing. Based on the experimental and theoretical work described above, shrinkage and/or light densification of the silicon carbide during the liquid silicon phase have been excluded as causes of the bulk surface overfilling in the SLS silicon-silicon carbide parts. Further investigation of the problem continues and may require a more kinematical approach.

5. References

Dutta, S. (1989) High-Strength Silicon Carbides by Hot Isostatic Pressing, ***Proceedings of the Third Symposium on Ceramic Materials and Components for Engines***, Las Vegas, V.J. Tennery, ed., The American Society, Inc., 683-695.

German, R.M. (1998) Consolidation Principles and Process Molding in ***ASM Handbook Volume 7: Powder Metal Technologies and Applications***, ASM International, Materials Park OH USA, 437-452.

Gern, F.H. (1995) Interaction Between Capillary Flow and Macroscopic Silicon Concentration in Liquid Siliconized Carbon/Carbon, ***Ceramic Transactions***, 58, 149.

Heady, R.B. and Cahn (1970) J.W., An Analysis of the Capillary Forces in Liquid-Phase Sintering of Spherical Particles, ***Metallurgical Transactions***, 1(1), 185-189.

Ko, T. (2000) Microstructural Changes of Phenolic Resin during Pyrolysis, ***J. Applied Polymer Science***, 81, 1084-1089.

Mortensen, A. and Cornie, J.S. (1987) On the Infiltration of Metal Matrix Composites, ***Metallurgical Transactions A***, 18A, 1160-1163.

Wang, H. (1999) ***Advanced Processing Methods for Microelectronics Industry Silicon Wafer Handling Components***, Ph.D. Dissertation, The University of Texas at Austin, Austin TX USA, 37-44.